Scanning tunneling microscopy of an Al-Ni-Co decagonal quasicrystal

M. Kishida,[1,2] Y. Kamimura,[1] R. Tamura,[2] K. Edagawa,[1,*] S. Takeuchi,[2] T. Sato,[3] Y. Yokoyama,[4] J. Q. Guo,[5] and A. P. Tsai[6]

[1]*Institute of Industrial Science, The University of Tokyo, Komaba, Meguro-ku, Tokyo 153-8505, Japan*

[2]*Department of Materials Science and Technology, Science University of Tokyo, Noda, Chiba 278-0022, Japan*

[3]*JEOL Ltd., Musashino, Akishima, Tokyo 196-8558, Japan*

[4]*Department of Materials Science and Engineering, Himeji Institute of Technology, Himeji, Hyougo 671-2201, Japan*

[5]*Japan Science and Technology Corporation, National Research Institute for Metals, Tsukuba, Ibaraki 305-0047, Japan*

[6]*National Research Institute for Metals, Tsukuba, Ibaraki 305-0047, Japan*

(Received 1 May 2001; revised manuscript received 18 September 2001; published 21 February 2002)

The structure of an Al-Ni-Co decagonal (*d*-) quasicrystal has been investigated by scanning tunneling microscopy (STM). STM images with atomic-scale resolution have been obtained successfully for the surfaces of both tenfold and twofold planes. On the tenfold surface, large terraces and monoatomic-layer steps are formed. The symmetry of each layer is not decagonal but pentagonal and the two adjacent layers are related by the inversion symmetry. The step lines are rough, which can be attributed to the existence of many symmetrically equivalent low-energy steps. The atom adsorptions are often observed at locally symmetric sites. An analysis based on the high-dimensional description of the quasicrystalline structure has shown that the structure has nearly perfect quasiperiodic order for the decagonal quasicrystal. On the twofold surface, interlayer phason defects are observed, but the density of them is quite low. This fact indicates that the *d*-quasicrystal of the present sample is not in the random tiling state in which the configurational entropy related to the phason disorder stabilizes the quasicrystal.

DOI: 10.1103/PhysRevB.65.094208 PACS number(s): 61.44.Br, 68.37.Ef

I. INTRODUCTION

Since the first discovery of a quasicrystal in an Al-Mn alloy by Shechtman *et al.*,[1] many theoretical and experimental works have been done for elucidating its complicated atomic structure. The experimental studies of the atomic structure of the quasicrystal done so far can be classified into two groups: one group consists of the studies by diffraction techniques using x-ray, electron, and neutron diffraction and the other those by microscopic techniques such as high-resolution transmission electron microscopy (HRTEM) and scanning tunneling microscopy (STM). As for the microscopic techniques, the former has been used much more frequently than the latter.

In principle, HRTEM gives information on the bulk structure in the sense that it images the average structure over the thickness of the sample, although in some particular cases it has also been used to probe the surface structure. In contrast, STM can probe directly the structure of a single atomic layer at the surface, and therefore it can give potentially the structural information that HRTEM cannot, although in STM we always have to examine the results carefully in view of the possible surface specifics such as surface reconstruction, compositional change, etc. In addition, STM can be more useful than HRTEM for investigating local defects such as phason defects,[2] which are possibly obscured in the average structure.

Reflecting the quasiperiodic translational order, quasicrystals have additional elastic degrees of freedom not found in conventional crystals, which are termed phason degrees of freedom.[2,3] The strain related to the phason degrees of freedom is called phason strain, which introduces a local atomic rearrangement called a phason defect or phason disorder.[2] Investigating the phason disorder is important because it could give an answer to the fundamental question as to why the quasicrystalline structural order is realized in material. At present, two distinct models have been proposed for the physical origin of the quasicrystalline structural order. One is the perfectly ordered quasiperiodic model, in which the quasicrystal is assumed to be energetically stabilized.[4,5] The other is the random tiling model, in which the quasicrystal is assumed to be stabilized by a configurational entropy related to the phason disorder.[6] At present, it is still controversial as to which of the two models better describes the quasicrystal in real material or whether it makes transitions between the two states with changing temperature. STM observations potentially give valuable information on this problem.

In 1990, Kortan *et al.*[7,8] reported STM observations with an atomic-scale resolution for an Al-Cu-Co decagonal (*d*-)quasicrystal. Since this pioneering work, several groups have performed STM observations of the surfaces of quasicrystals. Schaub *et al.*,[9,10] Shen *et al.*,[11] and Ledieu *et al.*[12,13] have presented atomic-scale resolution STM images of the surface of the Al-Pd-Mn icosahedral (*i*-)quasicrystal. Ebert *et al.*[14,15] have observed the cleaved surface of the *i*-Al-Pd-Mn and shown arrangement of atomic clusters. In contrast to a lot of these works on *i*-quasicrystals, very few STM works have been done so far on *d*-quasicrystals.[16] In this paper, we report structural studies of *d*-quasicrystals in the Al-Ni-Co system by STM. The Al-Ni-Co *d*-quasicrystal was discovered by Tsai *et al.*[17] as a thermodynamically stable phase. For this phase, centimeter-sized single grains of good quality have been grown by a floating zone method[18] and by a Czochralski method.[19] In the present study, we observed the surface of the tenfold and twofold planes of those single-grained quasicrystals and succeeded in obtaining atomic-scale resolution images for both the two types of planes.

II. EXPERIMENTAL PROCEDURES

Single grains of Al-Ni-Co decagonal quasicrystal were grown by a floating zone method and also by a Czochralski method. The detailed procedures have been reported elsewhere.[18,19] No noticeable difference was detected between the samples prepared by the two different methods in the present experiments of scanning tunneling microscopy. The single grains grown have columnar shape with the normal axis parallel to the tenfold direction. The size of the columns is about 15 mm in length and 7 mm in diameter for the grains grown by the floating zone method and about 30 mm in length and 3 mm in diameter for those grown by the Czochralski method. It was confirmed by x-ray Laue photography and x-ray diffractometory that the columns consist entirely of single grain of decagonal quasicrystal with high structural perfection. Two types of surfaces were prepared for STM observations: the surface perpendicular to the tenfold direction and that perpendicular to a twofold direction. Here the twofold direction is one of the ten twofold directions perpendicular to the tenfold direction. The samples were cut perpendicularly to the respective directions and the surfaces were polished mechanically to optical flatness. The misorientation of the surface from each symmetry axis was to within 5°.

STM experiments were performed using a JEOL JSTM-4610 scanning tunneling microscope system equipped with an ultrahigh-vacuum (UHV) chamber with base pressure of about 2×10^{-8} Pa. The sample surface was cleaned by repeated cycles of ion bombardment (Ar^+ ions, 1 keV) and annealing at various temperatures up to 1173 K in the UHV chamber before STM observation. The STM observations were made at room temperature in the constant-current mode with various sample bias voltages of both signs.

III. RESULTS

Figure 1 shows a low-magnification STM image of the surface of the tenfold plane, where large terraces are observed. In the inset, the height profile along the line between *A* and *B* in the image is shown, indicating that the step height is 0.22 nm, where the estimated error is ±0.04 nm. As described in detail in the next section, it has been shown experimentally that the structure of the Al-Ni-Co decagonal quasicrystal basically consists of an alternate stacking of two types of flat atomic layers with a spacing of 0.204 nm.[26] Thus the step height observed here corresponds to the height of the monoatomic layer. We confirmed that all the steps have a monoatomic layer height of about 0.2 nm. The monoatomic layer step has been observed also in an Al-Cu-Co *d* phase by Kortan *et al.*[7] On the other hand, the terraces are atomically flat with a corrugation of less than 0.05 nm except for local protrusions (white spots seen in the image of Fig. 1) of about 0.2 nm. We notice that the step lines are not smooth or straight, but very rough.

Figure 2 shows an example of a high-magnification STM image on a single terrace. In this image, an atomic-scale resolution is attained, which is confirmed by inspecting the Fourier transform of the image. In Fig. 3, the Fourier transform is calculated numerically from the image in Fig. 2,

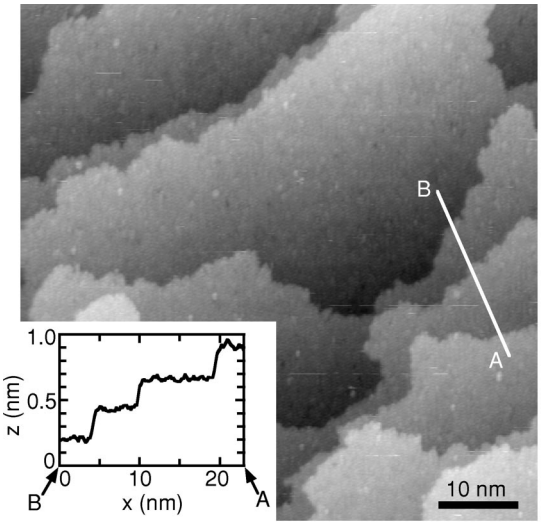

FIG. 1. Low-magnification STM image of the surface of the tenfold plane ($U_{\text{bias}}=0.10$ V, $I_{\text{tunnel}}=0.30$ nA), together with the height profile along the line between *A* and *B* indicated in the image. In the height profile, the inclination of the terrace area of about 1.1° is subtracted.

showing an arrangement of sharp spots with decagonal symmetry. Here the line profile between points *A* and *B* is shown in the lower part of Fig. 3. The peaks *P* and *Q* in the profile have *q* values of 9.9 ± 1.0 nm^{-1} and 15.8 ± 1.0 nm^{-1}, corresponding to the *d* values of 0.64 ± 0.06 nm and 0.40 ± 0.03 nm, respectively. It is noteworthy that these values have a ratio close to the golden mean $\tau[=(1+\sqrt{5})/2]$. The *d* values indicate that an ''atomic-scale'' resolution is attained, although it is still not the ''atomic resolution'' by which resolving individual atoms is meant. In the image in Fig. 2, one notices by looking at the image at grazing angle that mass-

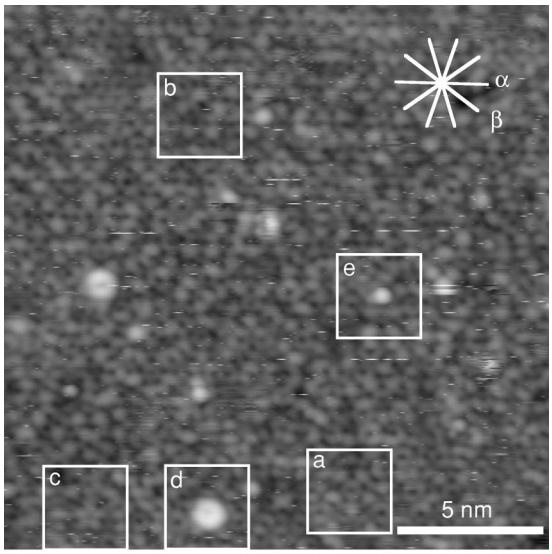

FIG. 2. High-resolution STM image of the surface of the tenfold plane ($U_{\text{bias}}=-0.40$ V, $I_{\text{tunnel}}=0.30$ nA). We find the patterns having local pentagonal symmetry, some of which are encircled. The patterns *a*–*e* are enlarged and presented in Fig. 5.

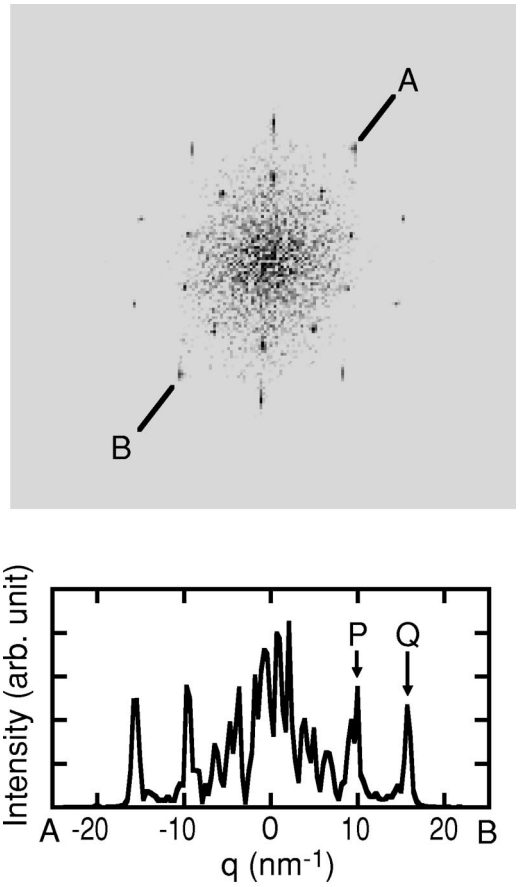

FIG. 3. Fourier transform calculated for the image of Fig. 2, together with the profile along the line between *A* and *B* in the figure.

density lines run along the decagonal symmetry directions shown in the image. Jogs of the lines, which should be observed in the presence of phason disorder, are not clearly noticed, although in some of the directions the lines themselves are not clear enough to conclude the absence of the phason disorder.

To examine translational order in the structure in the STM image of Fig. 2, we calculated one-dimensional functions defined as $f(x)=\int z(x,y)dy$, where $z(x,y)$ is the height function of the image and (x,y) are coordinates referred to two mutually orthogonal unit vectors $\mathbf{e}_x$ and $\mathbf{e}_y$. Here $\mathbf{e}_y$ is taken so that the direction of it coincides with one of the symmetry directions shown in Fig. 2. The functions $f(x)$ are calculated for the symmetry directions α and β in Fig. 2, which are presented in the lower parts of Figs. 4(a) and 4(b), respectively. Three different distances are found between adjacent peak positions, which can be written as $a_0\tau^n$, where a_0 is about 0.53 nm and $n=-1$, 0, or 1. As a result, the peak positions are reproduced by projecting a subset of the two-dimensional square lattice points onto the line with a slope of τ, as shown in the upper parts of Figs. 4(a) and 4(b). Here the two-dimensional lattice points yielding a part of the Fibonacci lattice are connected by line segments. The subset of the lattice points giving the peak positions experimentally observed consists of those yielding a part of the Fibonacci lattice and only a few more points nearby. This fact indicates

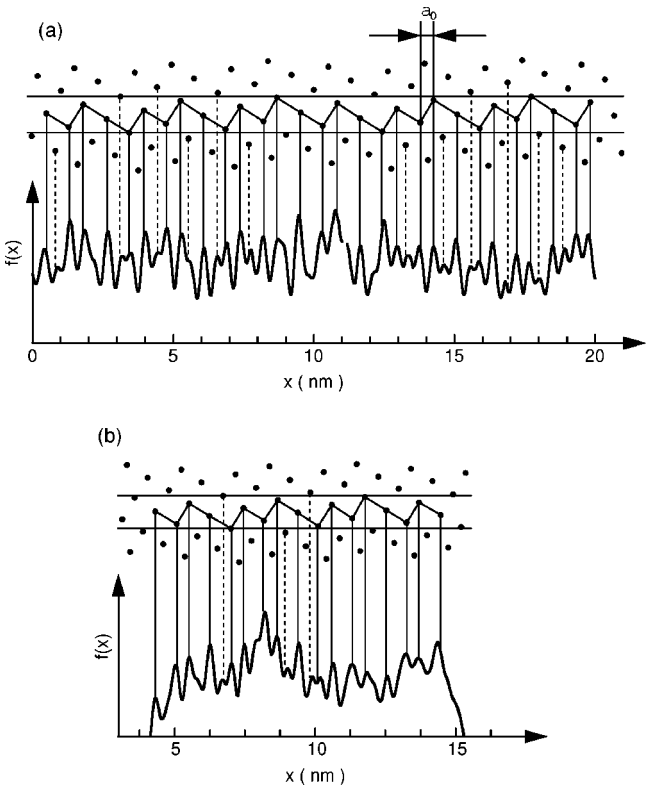

FIG. 4. Functions $f(x)$ defined in the text calculated from the image in Fig. 2. The functions in (a) and (b) are calculated for the symmetry directions α and β in Fig. 2, respectively. Three different distances are seen between adjacent peak positions, which can be written as $a_0\tau^n$ [$\tau=(1+\sqrt{5})/2$], where a_0 is about 0.53 nm and $n=-1$, 0, or 1. The peak positions are reproduced by projecting a subset of the two-dimensional square lattice points onto the line with the slope of τ. The two-dimensional lattice points yielding a part of the Fibonacci lattice are connected by line segments. The two horizontal parallel lines show the acceptance strip for generating the Fibonacci lattice.

the presence of a nearly perfect quasiperiodic order for the decagonal quasicrystal. Becker *et al.*[8] have previously applied essentially the same analysis for the STM image of *d*-Al-Cu-Co to obtain only a nearly periodic function. The origin of the different results is unclear, but it may indicate that in our observations better resolution is attained.

In the image in Fig. 2, we detect various types of patterns having local pentagonal symmetry. Examples of such patterns are encircled by square in Fig. 2, which are enlarged and shown in Figs. 5(a)–5(c). These patterns are repeated in the image. It should be noted that no patterns with local decagonal symmetry can be detected in the image.

In Figs. 5(d) and 5(e), local protrusions seen in Fig. 2 are enlarged and displayed. It is shown that these protrusions are located at the sites having local pentagonal symmetry. The tendency of the protrusions sitting at locally symmetric sites is confirmed by inspecting many images taken in the present experiments. For example, we find a protrusion sitting at the site having local pentagonal symmetry in the bottom part of the image in Fig. 7. In relation to this result, Ledieu *et al.*[20] have recently shown by STM that locally symmetric sites on

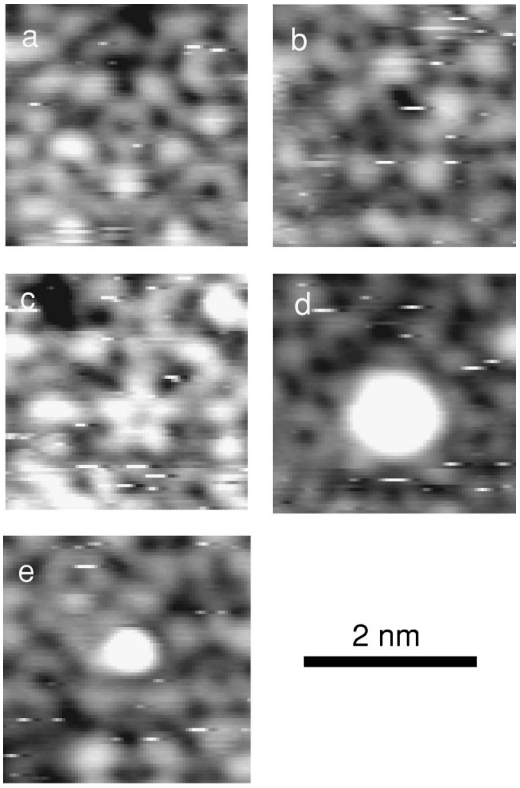

FIG. 5. Enlarged images of the patterns having local pentagonal symmetry ($a-c$) and those of local protrusions (d and e) observed in the image of Fig. 2.

the surface of *i*-Al-Pd-Mn function as adsorption sites for C_{60} molecules.

Figure 6 shows a high-magnification STM image, where pentagonal-star-shaped contrasts are seen most conspicuously. Some of the pentagonal-star contrasts are encircled in the figure. Here a striking feature to be noted is that the orientations of all the pentagonal stars are the same despite there being two possible orientations conforming to the global decagonal symmetry. This fact clearly indicates that the single atomic layer does not possess a tenfold symmetry, but only possesses a fivefold symmetry. It is worth noting here that the Fourier transform cannot distinguish between the tenfold and fivefold symmetries. In addition, we find that (1) many pentagonal stars are aligned in the symmetry directions and (2) the distances between the pentagonal stars have τ scalings. These facts clearly indicate that the pentagonal stars are arranged according to quasicrystalline order. In Fig. 7, a low-magnification STM image is presented, where two adjacent terraces are observed. In each terrace, arrangements of the same type of pentagonal star contrasts as those in Fig. 6 are shown. Here we find that (1) the pentagonal stars in the same terrace have the same orientation and (2) those in the adjacent terraces have the opposite orientations.

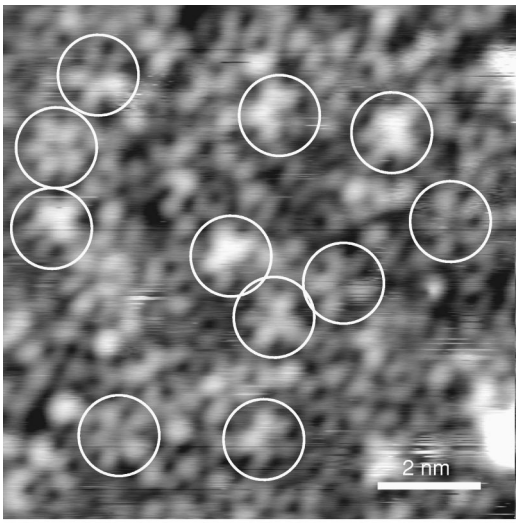

FIG. 6. High-resolution STM image of the surface of the tenfold plane ($U_{\mathrm{bias}}=-0.23$ V, $I_{\mathrm{tunnel}}=0.35$ nA). Pentagonal-star-shaped contrasts are seen most conspicuously, some of which are encircled. All the pentagonal stars orient in the same direction. They are aligned in the symmetry directions, and the distances between them have τ scalings.

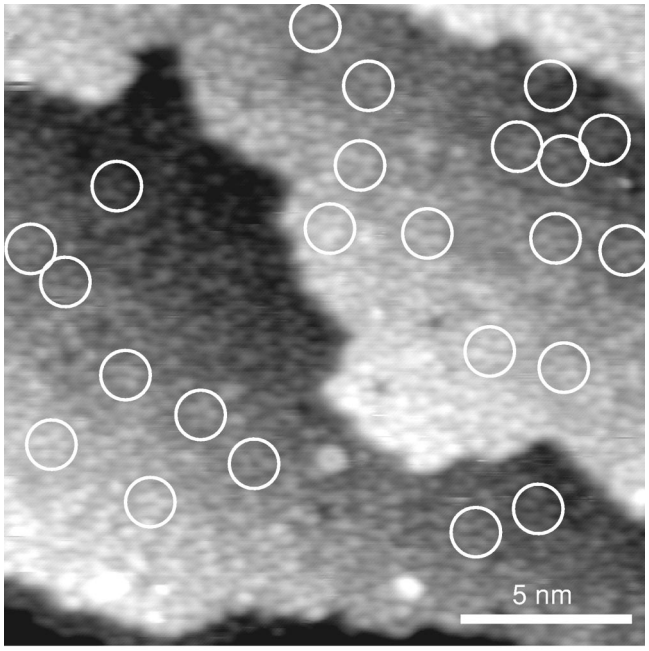

FIG. 7. Low-magnification STM image of the surface of the tenfold plane ($U_{\mathrm{bias}}=-0.21$ V, $I_{\mathrm{tunnel}}=0.30$ nA), where two adjacent terraces are observed. In each terrace, the arrangement of the same type of pentagonal star contrasts as those in Fig. 6 are shown, which are encircled. The pentagonal stars in the same terrace have the same orientation, and those in the adjacent terraces have the opposite orientations.

Figure 8 shows an STM image of the surface of the twofold plane, where terraces and steps are observed. In contrast to the steps on the surface of the tenfold plane in Fig. 1, the steps observed in Fig. 8 are straight; they orient exactly to the tenfold direction. In Fig. 9, the height profile along the line between points A and B in Fig. 8 is shown. Here the following points should be noted: (1) there are two different step heights $L=0.8\pm0.04$ nm and $S=0.5\pm0.04$ nm ($L/S\approx\tau$), as shown in the figure, and (2) the sequence of them is aperiodic. These are consistent with the fact that the

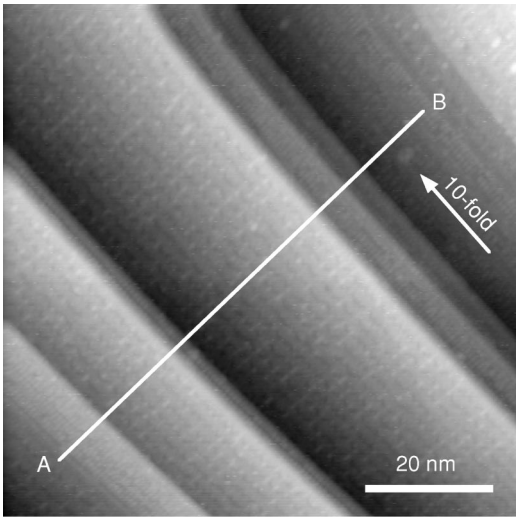

FIG. 8. Low-magnification STM image of the surface of the twofold plane ($U_{\text{bias}}=-0.08$ V, $I_{\text{tunnel}}=0.20$ nA). Large terraces and straight steps along the tenfold direction are observed. The height profile along the line between *A* and *B* is presented in Fig. 9.

decagonal quasicrystal has quasiperiodic order along the twofold direction. A similar observation has previously been reported for an Al-Pd-Mn icosahedral quasicrystal by Schaub *et al.*[9] They have found two kinds of step height with the ratio τ on the surface of a fivefold plane and shown that the sequence of them agrees with the Fibonacci sequence.

Figure 10 presents an example of a high-magnification STM image of the surface of the twofold plane, where an atomic-scale resolution is attained. Here many rows of white spots are observed to run along the tenfold direction. The rows are in parallel to each other and are arranged quasiperiodically in the direction perpendicular to the tenfold direction. In each row, the white spots are arranged periodically in the tenfold direction. Here it should be noted that there is a variety in the periodicity; the shortest periodicity of $a_0 \approx 0.4$ nm is seen, for example, in row *A* in Fig. 10, the second shortest periodicity of about $2a_0$ in row *B*, and the largest periodicity of about $3a_0$ in row *C*. In Fig. 11, height profiles for parts of the three types of atomic rows are shown for clarity. The bulk structure of the present phase has a periodicity of 0.4 nm along the tenfold direction, which agrees with the shortest periodicity observed here. The

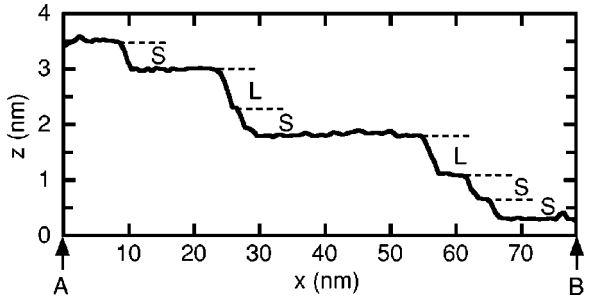

FIG. 9. Height profile along the line between *A* and *B* in the image in Fig. 8, where the inclination of the terrace area of about 2.6° is subtracted.

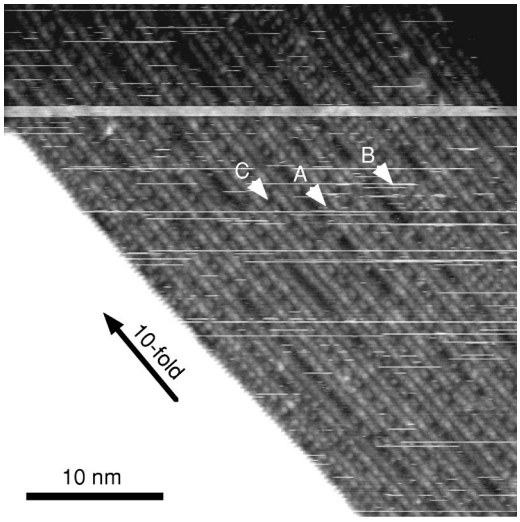

FIG. 10. High-resolution STM image of the surface of the twofold plane ($U_{\text{bias}}=-0.38$ V, $I_{\text{tunnel}}=0.20$ nA). Many rows of white spots run along the tenfold direction. The rows are in parallel to each other and are arranged quasiperiodically in the direction perpendicular to the tenfold direction. In each row, the white spots are arranged periodically in the tenfold direction. Three different periodicities can be detected: $a_0 \approx 0.4$ nm, $2a_0$, and $3a_0$, as observed in rows *A*, *B*, and *C*, respectively.

double and triple periodicities observed may be attributed to surface reconstruction.

The interlayer phason defects, which should yield jogs in the row, are not observed in the image in Fig. 10. Here what is meant by the interlayer phason defect is the defect in which a phason flip occurs between the adjacent layers along

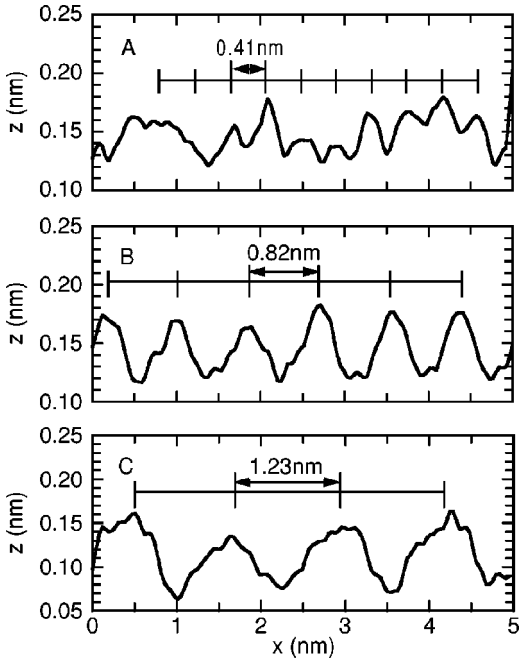

FIG. 11. Height profiles for parts of the three types of atomic rows shown in the image of Fig. 10, showing three different periodicities of about 0.41, 0.82, and 1.23 nm.

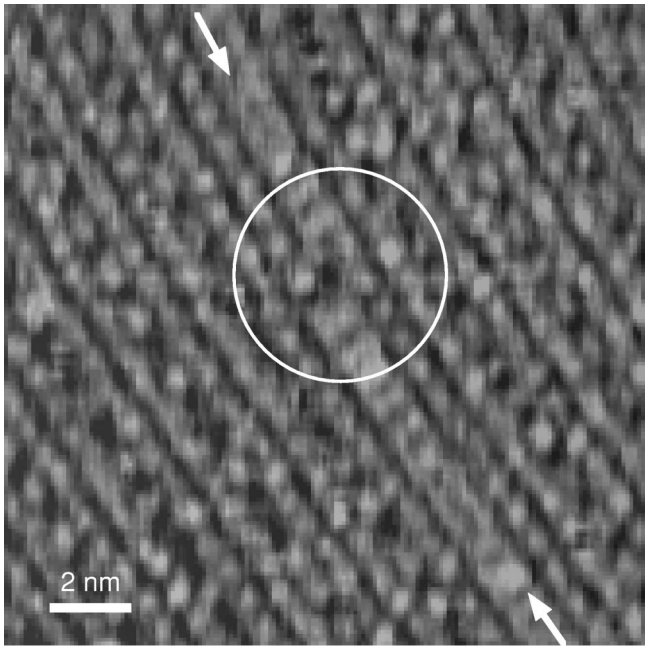

FIG. 12. High-magnification STM image of the surface of the twofold plane ($U_{\mathrm{bias}}=-0.63$ V, $I_{\mathrm{tunnel}}=0.20$ nA), in which a phason defect is observed at the position encircled. The row indicated by an arrow runs along the tenfold direction, terminates at the position encircled, shifts by a small amount, and runs again in the same direction. This corresponds to an interlayer phason defect in which a phason flip occurs between the adjacent layers along the tenfold direction.

the tenfold direction.[6,21] Compared with the mass-density lines in the image of the surface of the tenfold plane in Fig. 2, the rows of white spots along the tenfold direction in Fig. 10 are much more clearly observed. Therefore, we can conclude that the interlayer phason defects are really absent in the image of Fig. 10. An example of the interlayer phason defect observed is presented in Fig. 12. The row indicated by an arrow runs along the tenfold direction, terminates at the position encircled, and runs again in the same direction. However, this type of phason defect was very rarely observed in the present sample; the number density of it was less than 2×10^{-4} nm^{-2}. Here we should stress that the evaluation of the density of the phason defect is quite difficult by HRTEM because it images the projection of the structure.

IV. DISCUSSION

It has been well established that the surface of a solid is not a simple cut of the bulk: the structure and composition are usually different from those in the bulk. Unfortunately, in the present experiment, other techniques for surface characterization such as photoemission spectroscopy, Auger electron spectroscopy, etc., were not available, and we cannot say anything about the compositional change at the surface from that of the bulk. (Detailed surface characterizations have been performed for isocahedral Al-Pd-Mn alloys.[9,22,23]) However, as far as the structure is concerned, the overall features in the surface structure observed by STM in the present experiments reflect well the structure in the bulk except for an indication of surface reconstruction on the twofold plane, as shown in Fig. 10; the surface structures observed are consistent with the bulk structure previously characterized by various techniques, as described below.

The atomic structure of the Al-Ni-Co *d*-quasicrystal (or that of Al-Cu-Co *d*-quasicrystal isostructural with it) has been investigated by x-ray diffraction,[24–26] by conventional electron diffraction,[27,28] by convergent beam electron diffraction (CBED),[29,30] by high-resolution transmission electron microscopy,[27,29,31–35] and by high-angle dark-field scanning transmission electron microscopy (HADDF-STEM).[36–38] The space group has been determined by CBED to be $P10_5/mmc$ (Ref. 29) except for a few melt-quenched samples which show the space group of $P\overline{10}m2$.[30] Many structure models having the space group of $P10_5/mmc$ have been proposed.[26,35,38,39–43] The structure has been shown to consist of an alternate stacking of two types of flat atomic layers (*A* and *B*) in the tenfold direction with an identical spacing of 0.2 nm, making up a periodicity of 0.4 nm. Each layer of *A* and *B* has a pentagonal symmetry of $5m$, and they are related by inversion symmetry. The quasilattice constant of the two-dimensional quasicrystal in the layer is 0.246 nm.

The reciprocal basis vectors necessary for indexing diffraction peaks for the decagonal quasicrystal are given by $\mathbf{p}_i=a(\cos(2\pi i/5),\sin(2\pi i/5),0)$ $(i=1,2,3,4)$ and $\mathbf{p}_5=(0,0,c)$, where the first four vectors are for the two-dimensional quasiperiodic plane and the last one is for the tenfold periodic direction. For *d*-Al-Ni-Co, *a* is calculated from the quasilattice constant of 0.246 nm to be 10.2 nm^{-1}. Using the basis vectors $\mathbf{p}_i=a(\cos(2\pi i/5),\sin(2\pi i/5),0)$ $(i=1,2,3,4)$ with $a=10.2$ nm^{-1}, the ten-ring spots including spot *P* and those including spot *Q* in the Fourier pattern in Fig. 3 are indexed as (1,0,0,0), etc., and (1,1,0,0), etc., respectively, i.e., the basis vectors necessary for the spots in the Fourier pattern of the surface structure are the same as those for the bulk structure. This fact indicates that the surface shown in Fig. 2 has essentially the same quasilattice structure as that in the bulk.

We observed exclusively the monoatomic step height of about 0.2 nm on the surface of the tenfold plane, as shown in Fig. 1. This is consistent with the alternate stacking structure of layers *A* and *B* mentioned above because the termination by layers *A* and *B* are equivalent. However, the two-layer step height has recently been observed for an Al-Ni-Co *d* phase by Cox *et al.*,[16] the reason for which is unclear. The pentagonal symmetry of each layer and the inversion relation between the adjacent two layers, which has been deduced from the results of diffraction experiments, are directly observed in the present experiments (Figs. 6 and 7). It is worth noting that in principle HRTEM cannot observe them because it images the projection of the structure. To discuss the atomic structure in more detail by comparing the observed image with the structural models proposed previously, we need the atomic resolution which is not attained in the present observation.

It is shown in Fig. 1 that the step line on the surface of the tenfold plane is rough. In Fig. 13, a high-resolution STM image of a step edge is presented. In the figure, the tenfold symmetry axes identified by the structure on the terrace are

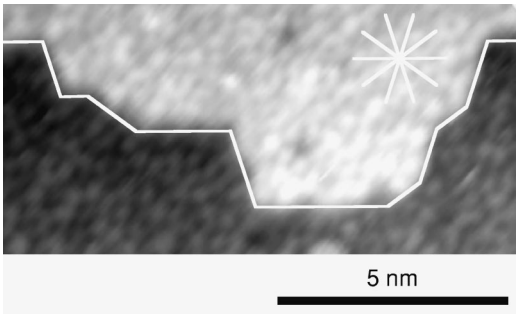

FIG. 13. STM image of a step on the surface of the tenfold plane ($U_{\mathrm{bias}}=-0.21$ V, $I_{\mathrm{tunnel}}=0.30$ nA). The tenfold symmetry axes identified by the structure on the terrace are also shown.

also shown. Here we notice that the step edge segments are mostly parallel to any of the symmetry directions. The rough step lines such as those shown in Fig. 1 are composed of the step edge segments parallel to the tenfold symmetry directions. Thus the formation of rough and largely wandering steps is considered to result from the existence of many symmetrically equivalent low-energy steps; the entropy gained by the step wandering overcomes the energy cost by the increase in the total length of the step. To quantify the properties of the steps, we applied the continuum step model and evaluated the step stiffness.[44] In the model, each of the steps is treated as a string whose energy is given by $E=(\tilde{\beta}/2)\int[\partial x(y)/\partial y]^2 dy$, where $\tilde{\beta}$ is the step stiffness and $x(y)$ is a coarse-grained step configuration. The mean-square displacement as a function of distance y, $G(y)=\langle|x(y)-x(0)|^2\rangle$ is expected to have the form $G(y)=kTy/\tilde{\beta}$ for an isolated step. Though the interaction between steps may not be negligible for the steps observed in the present experiment, we made a rough estimation of the step stiffness by use of the above equation. We deduced $G(y)$ for many steps and obtained roughly linear relations of $G(y)$ against y for all the steps analyzed. From the linear coefficients, we evaluated $\tilde{\beta}$ values, which range 3–50 meV/nm. These values are slightly smaller than those for the steps in Si (Refs. 45–47) and much smaller than those for metals such as Pt (Ref. 48) and Cu (Refs. 49 and 50). In contrast to the largely wandering steps on the tenfold surface, the steps on the twofold surface are straight; they orient exactly to the tenfold direction. This fact indicates that the step edge with this orientation is by far more stable than those with other orientations and that the kink formation costs much energy. The large energy cost for the kink formation indicates the large step stiffness in the continuum step model.

As described in the first section, two competing models have been proposed for the physical origin of the quasicrystalline structural order: the energetically stabilized perfectly ordered model[4,5] and the entropically stabilized random tiling model.[6] According to the latter model, a good amount of phason defects must be introduced three dimensionally because the entropy must be proportional to the volume of the system to overcome the energy of the system which grows three dimensionally. This indicates that in the case of the *d*-quasicrystal interlayer phason defects are required to be introduced as well as the intralayer phason defects.[6,21] As presented in Fig. 12, we observed the interlayer phason defects. However, the density of them was found to be quite low ($\approx 2\times 10^{-4}$ nm^{-2}). If we are allowed to assume that the density of the phason defects at the surface reflects faithfully the density in the bulk, this result leads to the conclusion that the *d*-quasicrystal of the present sample is not in accordance with the entropically stabilized random tiling model. Recently, we observed the motion of the phason flips in an *d*-Al-Cu-Co directly by *in situ* high-temperature HRTEM with the incident beam parallel to the tenfold direction.[51] In the experiments, we observed frequent phason jumps with the distance of 1.2 nm at temperatures above 1123 K, indicating that the thermal-equilibrium density of the interlayer phason defects is considerably high at high temperatures and that the very low density observed by STM reflects an equilibrium state at a lower temperature.

V. CONCLUSIONS

The surfaces of both tenfold and twofold planes of an Al-Ni-Co decagonal quasicrystal were examined by STM. For both surfaces, STM images with atomic-scale resolution were successfully obtained. On the tenfold surface, large terraces and monoatomic layer steps were observed to be formed. We found that the symmetry of each layer is not decagonal but pentagonal and that the two adjacent layers are related by the inversion symmetry. The step lines were rough, which can be attributed to the existence of many symmetrically equivalent low-energy steps. Adopting the continuum step model, we evaluated the step stiffness, which range 3–50 meV/nm. These values are slightly smaller than those for Si and much smaller than those for metals such as Pt and Cu. The atom absorptions were often observed at locally symmetric sites. An analysis based on the high-dimensional description of the quasicrystalline structure showed that the structure has nearly perfect quasiperiodic order for the decagonal quasicrystal. On the twofold surface, straight step lines along the tenfold direction were observed. This indicates that the step edge with this orientation is by far more stable than those with other orientations and that the kink formation costs much energy. Here we found an aperiodic sequence of two different step heights. On the twofold surface, many rows of white spots were observed along the tenfold direction. Here three types of rows were found, showing different periodicities $a_0\approx 0.4$ nm, $2a_0$, and $3a_0$, respectively. The latter two periodicities can be interpreted as due to surface reconstruction. Interlayer phason defects were observed, but the density of them was found to be quite low. This fact indicates that the decagonal quasicrystal of the present sample is not in the random tiling state in which configurational entropy related to phason disorder is assumed to stabilize the quasicrystal.

ACKNOWLEDGMENTS

We thank Professor T. Suzuki of IIS, University of Tokyo for valuable comments. This work has been partly supported by Core Research for Evolutional Science and Technology, Japan Science and Technology Corporation.

*Corresponding author.
Electronic address: edagawa@iis.u-tokyo.ac.jp

[1] D. Shechtman, I. Blech, D. Gratias, and J. W. Cahn, Phys. Rev. Lett. **53**, 1951 (1984).
[2] J. E. S. Socolar, T. C. Lubensky, and P. J. Steinhardt, Phys. Rev. B **34**, 3345 (1986).
[3] P. Bak, Phys. Rev. B **32**, 5764 (1985).
[4] D. Levine and P. J. Steinhardt, Phys. Rev. B **34**, 596 (1986).
[5] P. J. Steinhardt and H.-C. Jeong, Nature (London) **382**, 431 (1996).
[6] For a review, see C. L. Henley, in *Quasicrystals: The State of the Art*, edited by D. P. DiVincenzo and P. J. Steinhardt (World Scientific, Singapore, 1991), p. 111.
[7] A. R. Kortan, R. S. Becker, F. A. Thiel, and H. S. Chen, Phys. Rev. Lett. **64**, 200 (1990).
[8] R. S. Becker, A. R. Kortan, F. A. Thiel, and H. S. Chen, J. Vac. Sci. Technol. B **9**, 867 (1991).
[9] T. M. Schaub, D. E. Buergler, H.-J. Guentherodt, and J. B. Suck, Phys. Rev. Lett. **73**, 1255 (1994).
[10] T. M. Schaub, D. E. Buergler, H.-J. Guentherodt, J. B. Suck, and M. Audier, Appl. Phys. A: Mater. Sci. Process. **61**, 491 (1995).
[11] Z. Shen, C. Stoldt, C. Jenks, T. Lograsso, and P. A. Thiel, Phys. Rev. B **60**, 14 688 (1999).
[12] J. Ledieu, A. W. Munz, T. M. Parker, R. McGrath, R. D. Diehl, D. W. Delaney, and T. A. Lograsso, Surf. Sci. **433/435**, 665 (1999).
[13] J. Ledieu, R. McGrath, R. D. Diehl, T. A. Lograsso, D. W. Delaney, Z. Papadopolos, and G. Kasner, Surf. Sci. Lett. **492**, L729 (2001).
[14] Ph. Ebert, M. Feuerbacher, N. Tamura, M. Wollgarten, and K. Urban, Phys. Rev. Lett. **77**, 3827 (1996).
[15] Ph. Ebert, F. Yue, and K. Urban, Phys. Rev. B **57**, 2821 (1998).
[16] E. J. Cox, J. Ledieu, R. McGrath, R. D. Diehl, C. J. Jenks, and I. Fisher, in *Quasicrystals—Preparation, Properties, and Applications*, edited by E. Belin-Ferre, P. A. Thiel, A. P. Tsai, and K. Urban, MRS Symposia Proceedings No. 643 (Materials Research Society, Pittsburgh, 2001), K11.3.
[17] A. P. Tsai, A. Inoue, and T. Masumoto, Mater. Trans., JIM **30**, 150 (1989).
[18] T. J. Sato, T. Hirano, and A. P. Tsai, J. Cryst. Growth **191**, 545 (1998).
[19] Y. Yokoyama, R. Note, A. Yamaguchi, A. Inoue, K. Fukaura, and H. Sunada, Mater. Trans., JIM **40**, 123 (1999).
[20] J. Ledieu, C. A. Muryn, G. Thornton, R. D. Diehl, T. A. Lograsso, D. W. Delaney, and R. McGrath, Surf. Sci. **472**, 89 (2001).
[21] H. C. Jeong and P. J. Steinhardt, Phys. Rev. B **48**, 9394 (1993).
[22] M. Gierer, M. A. Van Hove, A. I. Goldman, Z. Shen, S.-L. Chang, C. J. Jenks, J. W. Anderegg, C.-M. Zhang, W. B. Chin, and P. A. Thiel, Phys. Rev. B **57**, 7628 (1998).
[23] C. J. Jenks, in *Quasicrystals*, edited by J. M. Dubois, P. A. Thiel, A.-P. Tsai, and K. Usban, MRS Symp. Proceedings No. 553 (Materials Research Society, Pittsburgh, 1999), p. 219.
[24] W. Steurer and K. H. Kuo, Philos. Mag. Lett. **62**, 175 (1990).
[25] W. Steurer, T. Haibach, and B. Zhang, Acta Crystallogr., Sect. B: Struct. Sci. **B49**, 661 (1993).
[26] A. Yamamoto, K. Kato, T. Shibuya, and S. Takeuchi, Phys. Rev. Lett. **65**, 1603 (1990).
[27] K. Edagawa, H. Tamaru, S. Yamaguchi, K. Suzuki, and S. Takeuchi, Phys. Rev. B **50**, 12 413 (1994).
[28] S. Ritsch, C. Beeli, H.-U. Nissen, T. Godecke, M. Scheffer, and R. Lueck, Philos. Mag. Lett. **78**, 67 (1998).
[29] K. Tsuda, Y. Nishida, K. Saitoh, M. Tanaka, A. P. Tsai, A. Inoue, and T. Masumoto, Philos. Mag. A **74**, 697 (1996).
[30] K. Saitoh, K. Tsuda, M. Tanaka, A. P. Tsai, A. Inoue, and T. Masumoto, Mater. Sci. Eng., A **181–182**, 805 (1994).
[31] K. Hiraga, F. J. Lincoln, and W. Sun, Mater. Trans., JIM **32**, 308 (1991).
[32] K. Hiraga and W. Sun, Philos. Mag. Lett. **67**, 117 (1993).
[33] K. Hiraga, in *Quasicrystals: The State of the Art* (Ref. 6), p. 429.
[34] C. Beeli, Mater. Sci. Eng., A **294–296**, 23 (2000).
[35] E. Abe, K. Saitoh, H. Takakura, A. P. Tsai, P. J. Steinhardt, and H.-C. Jeong, Phys. Rev. Lett. **84**, 4609 (2000).
[36] Y. Yan, S. J. Pennycook, and A. P. Tsai, Phys. Rev. Lett. **81**, 5145 (1998).
[37] K. Saitoh, K. Tsuda, M. Tanaka, K. Kaneko, and A. P. Tsai, Jpn. J. Appl. Phys., Part 2 **36**, L1400 (1997).
[38] P. J. Steinhardt, H.-C. Jeong, K. Saitoh, M. Tanaka, E. Abe, and A. P. Tsai, Nature (London) **396**, 55 (1998).
[39] S. Burkov, Phys. Rev. Lett. **67**, 614 (1991).
[40] T. L. Daulton, K. F. Kelton, and P. C. Gibbons, J. Non-Cryst. Solids **153&154**, 15 (1993).
[41] C. L. Henley, J. Non-Cryst. Solids **153&154**, 172 (1993).
[42] G. Zeger and H.-R. Trebin, Phys. Rev. B **54**, R720 (1996).
[43] K. Saitoh, K. Tsuda, and M. Tanaka, J. Phys. Soc. Jpn. **67**, 2578 (1998).
[44] For a review, see H.-C. Jeong and E. D. Williams, Surf. Sci. Rep. **34**, 171 (1999).
[45] N. C. Bartelt and R. M. Tromp, Phys. Rev. B **54**, 11 731 (1996).
[46] H. J. W. Zandvliet and B. Poelsema, Phys. Rev. B **51**, 5465 (1995).
[47] K. Sudoh, T. Yoshinobu, and H. Iwasaki, Phys. Rev. Lett. **80**, 5152 (1998).
[48] M. Giesen-Seibert, G. S. Icking-Konert, K. Stapel, and H. Ibach, Surf. Sci. **366**, 229 (1996).
[49] L. Barbier, L. Masson, J. Cousty, and B. Salanon, Surf. Sci. **345**, 197 (1996).
[50] L. Masson, L. Barbier, J. Cousty, and B. Salanon, Surf. Sci. **317**, L1115 (1994).
[51] K. Edagawa, K. Suzuki, and S. Takeuchi, Phys. Rev. Lett. **85**, 1674 (2000); and (unpublished).